Biochemical and Biophysical Research Communications 445 (2014) 299–303

Contents lists available at ScienceDirect

Biochemical and Biophysical Research Communications

journal homepage: www.elsevier.com/locate/ybbrc

A functional fragment of Tau forms fibers without the need for an intermolecular cysteine bridge

Isabelle Huvent [a], Amina Kamah [a], François-Xavier Cantrelle [a], Nicolas Barois [b], Christian Slomianny [c], Caroline Smet-Nocca [a], Isabelle Landrieu [a], Guy Lippens [a,*]

[a] CNRS UMR 8576, University of Lille1, 59655 Villeneuve d'Ascq, France
[b] Plate-forme BICeL-IFR142, Institut Pasteur de Lille, Lille, France
[c] Inserm U1003, Laboratoire de physiologie cellulaire, Université Lille 1, 59650 Villeneuve d'Ascq, France

ARTICLE INFO

Article history:
Received 21 January 2014
Available online 3 February 2014

Keywords:
Tau
Aggregation
Nucleation
Electron microscopy
NMR spectroscopy

ABSTRACT

We study the aggregation of a fragment of the neuronal protein Tau that contains part of the proline rich domain and of the microtubule binding repeats. When incubated at 37 °C with heparin, the fragment readily forms fibers as witnessed by Thioflavin T fluorescence. Electron microscopy and NMR spectroscopy show bundled ribbon like structures with most residues rigidly incorporated in the fibril. Without its cysteines, this fragment still forms fibers of a similar morphology, but with lesser Thioflavin T binding sites and more mobility for the C-terminal residues.

1. Introduction

Tau is a microtubule associated protein that promotes the association of tubulin units into microtubules (MTs) and further stabilizes microtubules [1]. It exists as a family of six different isoforms, that contain one or two inserts in its amino-terminal and three or four repeats in its C-terminal domain. Tight binding of these repeats together with the preceding proline rich region (PRR) are required for this MT related function [2], and the repeats have subsequently been named "microtubule binding repeats" (MTBRs). In Alzheimer's disease (AD), the same protein is found under a hyperphosphorylated and aggregated form, and forms the primary component of intraneuronal fibers [3–5].

Biochemical analysis of AD brain derived fibers allowed to define the MTBRs as the pronase inaccessible core of the fibers [6]. The three or four MTBR containing fragments were the first ones that yielded in vitro fibers after prolonged incubation in the absence of any poly-anionic aggregation enhancers, whereas full length Tau protein did not aggregate under the same conditions [7]. This first available model system further led to the notion that dimer formation by an intermolecular disulfide bridge of Cys322 in the third repeat is an absolute requirement for the nucleation of fiber formation. [8]. The discovery that poly-anionic factors such as heparin can not only accelerate significantly the aggregation process but equally lead to fibers from full-length Tau [9] allowed to further investigate the physical processes that lead to Tau aggregation, and confirmed that the intermolecular disulfide bridge is a determining factor for fiber formation starting from full-length Tau protein [10]. Recently, the mechanistic basis of methylene blue as an aggregation inhibitor was assigned to specific modifications to the native cysteines of Tau [11], further crediting the important role of this disulfide bridge formation in the nucleation process.

Fragments limited to only the MTBRs do however not capture completely the physiological or pathological aspects of Tau. Not only do they bind significantly less tightly to the MT surface, with a resulting reduced efficacy to assemble MTs from tubulin [2,12], the finding that certain phosphorylation events outside the MTBRs influence the aggregation clearly suggests that other regions of Tau equally regulate this process. As an example, phosphorylation of Ser214 in the PRR by the PKA kinase reduces MT binding but equally strongly suppresses the aggregation potential of Tau [13], whereas phosphorylation at the neighbouring Thr212 site would enhance the aggregation kinetics of Tau [14]. Further studies with N- or C-terminal truncated Tau fragments have suggested an aggregation inhibitory role for the C-terminal part [15] whereas removal of even a few residues in the extreme N-terminal part reduces the extent and rate of Tau polymerization [16]. Using a *de novo* screen of Tau fragments that bind to a soluble tubulin construct, we recently identified TauF4 (Tau208–324) as a fragment that binds more tightly to the MT surface as full-length Tau and stimulates very efficiently the assembly of tubulin [17]. The

* Corresponding author. Fax: +33 3 20 43 65 55.
E-mail address: Guy.Lippens@univ-lille1.fr (G. Lippens).

http://dx.doi.org/10.1016/j.bbrc.2014.01.161
0006-291X/

resulting MTs are however bundled, in agreement with the role of molecular spacer that was previously determined for the N-terminal projection domain [18]. Our fragment spans part of the PRR, the first two MTBRs and the part of the third repeat that by solid state NMR was delineated as the most rigidly embedded fragment in a 3-repeat construct derived fibers [19]. As it thereby contains the two hexapeptide motifs (PHF6 and PHF6*) that are thought to be the nuclei of the aggregation process [20,21], we decided to study its heparin induced aggregation process.

The C-terminal fragment is an effective barrier against aggregation [15] whereas the N-terminal projection domain has a stimulatory effect [16]. We find that the aggregation of our fragment devoid of both N- and C-terminal fragments sets in more rapidly than that of full-length Tau,. To investigate whether the intermolecular disulfide bridge postulated as an essential factor for the nucleation of full-length Tau fiber formation can be overcome by our shorter fragment, we study the aggregation process of TauF4 lacking any cysteines. Surprisingly, we find that TauF4 (C2S) still forms fibers on a rapid time scale. Similar as the TauF4 assembled MTs, these fibers do tend to clump together, eventually forming large aggregates. Characterization of the resulting fibers by electron microscopy and NMR spectroscopy leads to the conclusion that although the overall morphology of the resulting fibers is independent of the presence of the cysteines, the latter do have an influence on the packing of the Tau fragment in the fiber core.

2. Materials and methods

2.1. Cloning and site-directed mutagenesis

The coding region of the full-length 441-residue Tau protein was inserted into a pET15b expression vector (Novagen) as described previously, to produce a recombinant protein without any tag [22]. For the protein fragments i.e. F4 and F4 C291S, C322S (C2S), the cDNA for Tau-(S^{208}–S^{324}) (F4) was subcloned in pET15b between the restriction sites *Nco*I and *Xho*I using a primer encoding a 6 His-tag. The site-directed mutations of C to S were obtained by polymerase chain reaction (PCR) amplification with appropriate mutagenic primers. TauF4 constructs thereby include a short N-terminal His-tag (MGHHHHHH) to facilitate purification. The sequences of these constructs were verified by DNA sequencing.

2.2. Production of ^{15}N-labeled Tau and Tau-F4 fragments in Escherichia coli

Recombinant full-length human Tau (441 AA) and its fragments Tau F4 and Tau F4(C2S) were expressed in *Escherichia coli* BL21 (DE3) pLysS strain. Cells were grown at 37 °C in a M9 minimal medium containing 1 g/L ^{15}N-ammonium chloride, 4 g/L glucose, 1 mM MgSO4, 100 μM $CaCl_2$, Isogro® 0.5 g/L (Cortecnet), MEM vitamine cocktail (Sigma–Aldrich) and ampicilline (100 mg/L). The production of the proteins was initiated by adding 0.4 mM Isopropyl-1-thio-β-D-galactopyranoside (IPTG) to the bacterial cultures grown to an A_{600} of 0.8 and continued at 37 °C for 2 h. The cultures were centrifuged and the pellets were resuspended in the appropriate buffer: For the full-length protein (Tau441), the pellet was resuspended immediately in buffer A_1 (50 mM NaPi, 2.5 mM EDTA, pH 6.2). For the truncated proteins, the pellet was resuspended in buffer A_2 (50 mM NaPi, 300 mM NaCl, 20 mM imidazole, pH 7.6). Both buffers were complemented with 0.5 mM DTT, Triton 0.25% and a tablet of protease inhibitor cocktail (Complete™, Roche Applied Science). The soluble extracts were obtained by incubation of the cell suspension at 4 °C for 20 min with 0.3 mg/mL lysozyme and 0.03 mg/mL of DNase I, followed by a sonication step and centrifugation at 25,000*g* during 30 min. The supernatants were submitted to a heating at 75 °C for 15 min and the insoluble materials were removed by centrifugation for 20 min at 25,000*g*.

The extract corresponding to full-length construct was loaded on a Hi-Trap™ SP FF (GE Healthcare) equilibrated with buffer A_1 while the F4 and F4 (C2S) protein mixtures were purified to homogeneity by Ni Sepharose chromatography (HiTrap™ Chelating HP, GE Healthcare) equilibrated in buffer A_2. Proteins were eluted by a gradient and fractions were collected at (50 mM NaPi, 2,5 mM EDTA, 500 mM NaCl, pH 6.2) in case of Tau441 and at (50 mM NaPi, 300 mM NaCl, 200 mM imidazole, pH 7.6) for the His-tagged TauF4 proteins. The purified proteins, checked by 12% denaturing polyacrylamide gel electrophoresis, were then exchanged to 50 mM ammonium bicarbonate buffer using a HiPrep™ 26/10 Desalting column (GE Healthcare) prior to lyophilization.

2.3. Fluorescence assay for aggregation kinetics

All Tau proteins were dissolved at 100 μM in the aggregation reaction buffer (NaPi 25 mM, NaCl 25 mM, EDTA 2.5 mM, pH 6.6). For the aggregation assays, protein concentrations were normalized based on their NMR two-dimensional heteronuclear correlation spectra [^{1}H,^{15}N]-HSQC acquired at 600 MHz. Tau proteins and heparin (Heparin sodium salt from porcine intestinal mucosa, H-3149, average MW = 18 kDa, Sigma–Aldrich) were mixed to a ratio of 4:1 in the aggregation buffer with final concentrations of 10 or 5 μM for Tau proteins supplemented with 0.3 mM dithiothreitol (DTT). Thioflavine T (ThT, Sigma–Aldrich) was extemporaneously prepared at 5 mM, filtered through 0.22 μm syringe filter and protected from light. It was added to a final concentration of 50 μM just before starting the aggregation measurement. All kinetic measurements were performed at 37 °C using a PHERAStar (BMG LABTECH GmbH, Ortenberg, Germany) fluorimeter. All experiments were performed in 96-well plates sealed with adhesive film to reduce evaporation. Aggregation was monitored for at least 17 h with measurement every 5 min in three independent experiments for each protein concentration. The ThT fluorescence intensity was detected at 490 nm after excitation at 440 nm.

The supernatants (2 μg) corresponding to non aggregated or aggregated samples of F4 and F4(C2S) obtained after centrifugation 1 h at 16,000 g were resolved for 1 h 30 min by a 15% denaturating polyacrylamide gel at 180 V and subjected to Coomassie blue staining.

2.4. Electron microscopy

At the end of the aggregation experiment, 10 μL of the sample was placed on a formvar grid 400 mesh hexagonal for 30 s. The sample on grid was washed with water two times. The sample on grid was stained with uranyl acetate 2% for 1 min. At each step, excess stain was removed by blotting with filter paper touched to the edge of the grid. Grids were observed using an electron microscope Hitachi H7500 operated at 80 kV.

2.5. NMR spectroscopy

NMR spectra of fibers of full-length Tau were recorded on a Bruker 600 MHz spectrometer as described earlier [23]. For TauF4 and TauF4 (C2S), 500 μl of the proteins at 50 μM concentration were aggregated overnight under the conditions described above (1:4 heparin:TauF4, 0.3 mM DTT). At this concentration, a large cloudy structure was visible in both samples, that rapidly sedimented on the bottom of the tube. We used extensive vortexing to dissolve the cloudy structure, and obtained a clear sample that proved stable during the NMR measurement at 293 K. The ^{1}H, ^{15}N HSQC

experiment was recorded with 256 scans per increment as a 2048 × 256 complex matrix, for a total measurement time of 21 h/sample. Reference spectra of TauF4 and TauF4 (C2S) were recorded under identical conditions, but with only 16 scans per increment.

3. Results and discussion

In order to compare the aggregation kinetics of full-length Tau (Tau441) and TauF4, we first carefully dosed both proteins by recording ^{1}H, ^{15}N HSQC experiments on both ^{15}N labeled protein samples and comparing the intensity of equivalent correlations. After adjusting both protein samples to the same concentration, we used the Thioflavin T assay to monitor over time the fiber formation after addition of heparin and incubation at 37 °C. For full-length Tau, we obtained half of the maximal ThT intensity after 4 h, and the final plateau after 7 h (Fig. 1). The aggregation kinetics depends on the concentration, as shown by the slower kinetics in a similar experiment with 5 μM of Tau441 (Fig. 1). ThT fluorescence in an experiment with TauF4 under the same conditions of protein, heparin and DTT concentration showed two differences. First, the initial slope was significantly steeper, with the half maximum being reached after one hour and the plateau after 2 h. Secondly, the plateau value itself was less pronounced, reaching roughly half of that obtained with Tau441 (Fig. 1). This first experiment points to an inhibition by the projection domain and/or the C-terminal 100 residues of the fiber nucleation step and to a reduction of ThT binding sites in the final fibers derived from the TauF4 fragment as compared to those obtained with Tau441.

We deposited the resulting samples after overnight incubation on formvar-coated copper grids, and observed them by transmission electron microscopy. Whereas for Tau441, we could easily detect long (>1 μm) paired helical filaments with an average width of 15 nm and a twist of 110–120 nm (Fig. 1c), most fibers composed of TauF4 showed up with a morphology of ribbon like structures, and were found in bundles (Fig. 1d). Fiber width was equally smaller, with an average value of 10 nm, although this latter was harder to determine in the bundles. We assigned the bundling to the absence of the projection domain acting as a spacer element, similar as was observed for TauF4 and microtubule bundling [17].

To further characterize the molecular mobility within the fibers, we prepared new samples from 50 μM ^{15}N labelled Tau441 or TauF4, and recorded their NMR spectrum before and after the aggregation process. At these concentrations, TauF4 formed large cloudy structures visible at the naked eye, leading us to vortex extensively the sample before introducing it in the NMR spectrometer at 25 °C. For Tau441, roughly 40% of the intensity remained in the first increment of the ^{1}H, ^{15}N HSQC spectrum, in agreement with the previously determined flexible regions in the fibers of Tau [23]. For the TauF4 fibers, however, the resulting spectrum was basically empty (Fig. 2), and this despite a recording with 256 scans per increment compared to 16 scans per increment for the free TauF4 sample. Only for some selected resonances such as A246, we could observe some residual signal (Fig. 2). The absence of signal firstly indicates that very little free TauF4 is remaining in solution. A gel filtration experiment confirmed the lack of soluble fragment after the aggregation. The empty NMR spectrum equally indicates that most if not all residues of TauF4 are rigidly integrated into the fiber structure.

The more rapid nucleation and elongation kinetics of TauF4 compared to Tau441 suggests that without the N- or C-terminal parts of Tau441, the aggregation process becomes more efficient. We hence wondered whether the requirement for the intermolecular cysteine bridge, as postulated by early in vitro studies on the K18 fragment containing only the MTBRs or on the full-length Tau441 protein [7,10], would still be valid for the TauF4 fragment. To investigate this, we prepared a TauF4 (C2S) fragment in which both cysteines were mutated into Serine residues. After dosing of the fragment by NMR, we compared the aggregation profiles as monitored by ThT.

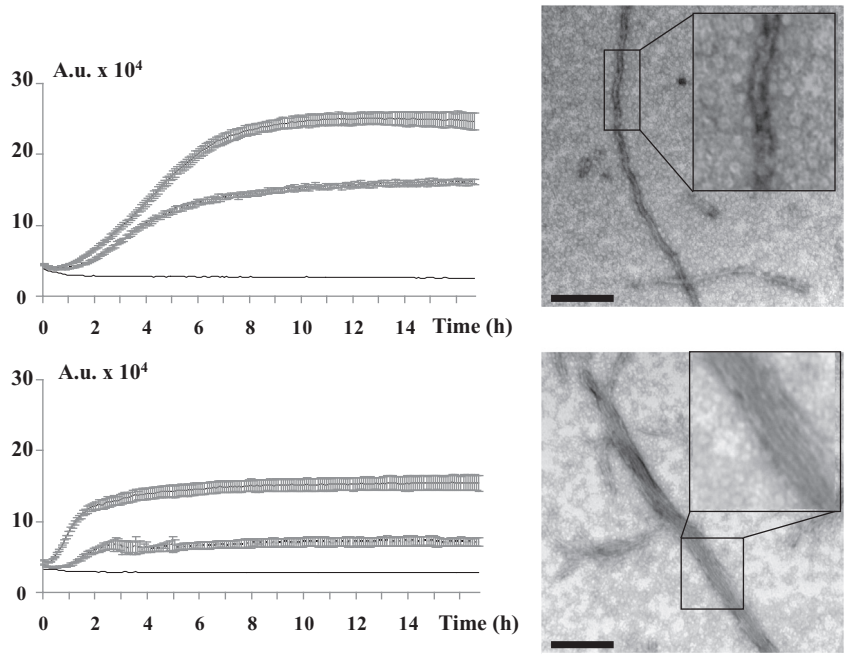

Fig. 1. Aggregation kinetics as followed by ThT fluorescence and electron microscopy images of the resulting fibers for Tau441 (top) and TauF4 (bottom). The kinetic experiments were performed at two concentrations of protein (10 and 5 μM, upper and lower curves), with the same protein without heparin as negative control (solid line). The error bars were derived from three independent experiments. Scale bar in the electron microscopy images presents 100 nm. The inserts are magnified 2×.

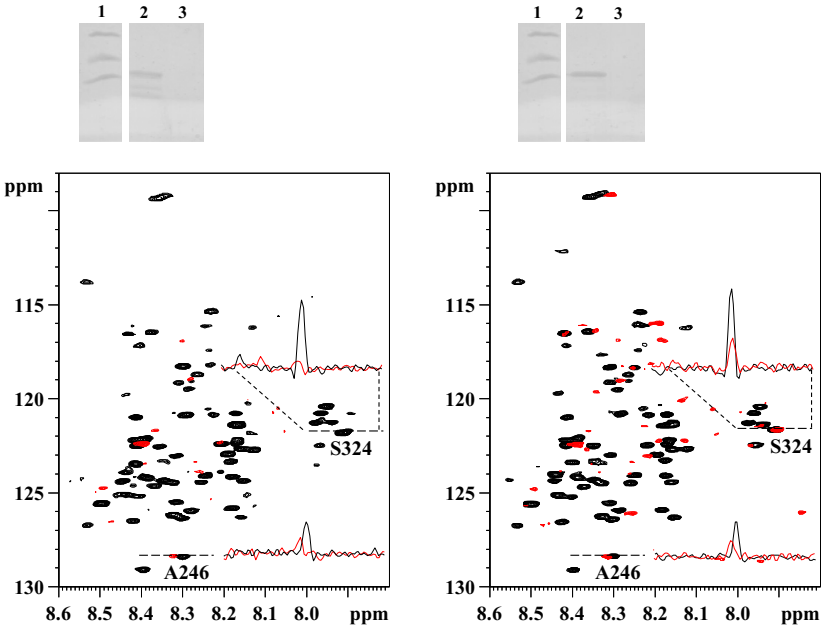

Fig. 2. (Top) SDS–Page of the TauF4 (left) or Tau F4 (C2S) samples before (lane 2) or after (lane 3) overnight aggregation. Molecular markers (lane 1) indicate molecular weights of 14, 18 and 25 kDa. (Bottom) ^{1}H, ^{15}N HSQC spectra of 50 μM of TauF4 (left) or TauF4 (C2S) (right) before (black) or after (red) aggregation. Inserts show the traces through the N-terminal A246 or C-terminal S324 resonances. (For interpretation of the references to colour in this figure legend, the reader is referred to the web version of this article.)

Tau F4 (2CS) does form amyloid structures as witnessed by the Thioflavin T response, but slower than Tau F4 (Fig. 3). Although already visible for the 10 μM experiment, the lag time for aggregation becomes important in the 5 μM sample, where aggregation only starts after 3 h. We thus conclude that the cysteine residues indeed accelerate the nucleation process, but that the primary sequence of Tau contains sufficient information to start the aggregation process at the condition that the counter-aggregation N- and/or C-terminal stretches are removed such as in TauF4.

The ThT fluorescence in the TauF4 (C2S) experiment does not reach the same level as in the equivalent TauF4 experiment (Fig. 3), suggesting that lesser ThT sites are formed. To evaluate whether this comes from less fibers (or, alternatively, to more free monomers in solution) or from fibers that do not present the same amount of ThT binding pockets per unit of fiber length, we first performed the gel filtration experiment and then again recorded the NMR spectrum after extensive vortexing of the cloudy aggregated TauF4 (C2S) sample (Fig. 2). No soluble TauF4 (C2S) could be detected in the gel of the aggregated sample (Fig. 2), and for residues in the first and second repeat, no intensity could be detected in the NMR spectrum, confirming the absence of an NMR detectable concentration of free monomers in solution. We did observe some intensity for residues both in the N- and C-termini of the fragment (Fig. 2). Residues such as A246 and M250, already visible in the spectrum of the wt TauF4 fibers but equally mobile in the solid state NMR spectra of the K19 fragment aggregated into fibers [19], could be assigned based on their proximity to the corresponding resonances in the spectrum of soluble TauF4 (Fig. 2). The C-terminal Ser324 resonance, however, could only be identified in the spectrum of TauF4 (C2S) but was completely absent from the spectrum of the fibers of wt TauF4. This indicates that beyond assisting the nucleation step, the presence of a cystein bridge equally stabilizes the molecular scaffold of the fibers and contributes to the structuration of the ThT binding pockets. Under the electron microscope, this aspect of greater flexibility did however not show up, and we again observed flat ribbon-like filaments of

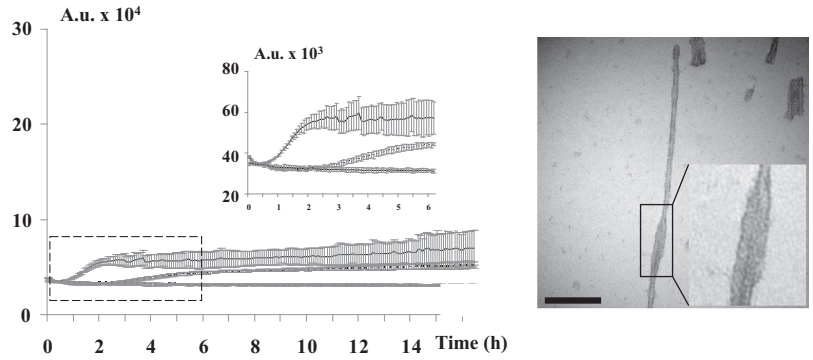

Fig. 3. Aggregation kinetics of TauF4 (C2S) as monitored by Thioflavin T fluorescence (left) and resulting electron microscopy image (right). The kinetic experiments were performed at two concentrations of protein (10 and 5 μM, upper and lower curves), with the same protein without heparin as negative control (solid line). The error bars were derived from three independent experiments. The box in the ThT profile is zoomed in the insert, to better show the delayed nucleation at 5 μM protein concentration. Scale bar in the electron microscopy image presents 100 nm. The insert is magnified 2×.

~10 nm width that stack together as pairs or higher order structures, and only occasionally show a twist (see insert Fig. 3).

In conclusion, the TauF4 fragment is not only functional as far as tubulin assembly concerns [17], but our present work shows that it can also form fibers as detectable by ThT fluorescence. The lack of projection domain that was previously found to lead to bundling of the assembled microtubules also translates in the bundling of the resultant ribbon-like structures. These latter ribbons do lack the fuzzy coat that is characterizing brain derived or synthetic fibers made with full-length Tau. Whereas full-length Tau critically depends on the presence of at least the Cys322 to start the nucleation process [7], TauF4 can efficiently nucleate the aggregation process even when both its cysteines are mutated, although the resulting fibers offer less Thioflavin T binding sites than those formed with the fragment containing the cysteines. The present TauF4 fragment hence should be a suitable tool to investigate the mechanistic aspects of potential aggregation inhibitors that would act independent of the cysteines.

Acknowledgments

We thank Drs. A. Leroy, J. Lopez (Lille, France), B. Chambraud, E.E. Baulieu, J Giustiniani, (Kremlin-Bicêtre, France) A.-M. Chollet, G. de Nanteuil, P. Lestage C. Mannoury la Cour, F. Panayi (Institut de Recherche Servier, Croissy, France) for insightful discussions. IH was financed by a research contract with the Institut de Recherche Servier (Croissy, France). The research leading to these results was supported by the Centre National de la Recherche Scientifique, the Agence Nationale de la Recherche (ANR-05-Blanc-6320-01 and program MALZ-TAF), the LABEX (Laboratory of Excellence - Program Investment for the Future) DISTALZ grant (Development of Innovative Strategies for a Transdisciplinary Approach to ALZheimer's disease), and the CNRS Large Scale Facility NMR THC Fr3050. The NMR facility is funded by the European Community, the CNRS, the Région Nord-Pas de Calais (France), the University of Lille 1, and the Institut Pasteur de Lille.

References

[1] D.W. Cleveland, S.Y. Hwo, M.W. Kirschner, Purification of Tau, a microtubule-associated protein that induces assembly of microtubules from purified tubulin, J. Mol. Biol. 116 (1977) 207–225.

[2] N. Gustke, B. Trinczek, J. Biernat, E.M. Mandelkow, E. Mandelkow, Domains of Tau protein and interactions with microtubules, Biochemistry (Mosc.) 33 (1994) 9511–9522.

[3] K.S. Kosik, C.L. Joachim, D.J. Selkoe, Microtubule-associated protein Tau (Tau) is a major antigenic component of paired helical filaments in Alzheimer disease, Proc. Natl. Acad. Sci. U.S.A. 83 (1986) 4044–4048.

[4] I. Grundke-Iqbal, K. Iqbal, M. Quinlan, Y.C. Tung, M.S. Zaidi, H.M. Wisniewski, Microtubule-associated protein Tau. A component of Alzheimer paired helical filaments, J. Biol. Chem. 261 (1986) 6084–6089.

[5] I. Grundke-Iqbal, K. Iqbal, Y.C. Tung, M. Quinlan, H.M. Wisniewski, L.I. Binder, Abnormal phosphorylation of the microtubule-associated protein Tau (Tau) in Alzheimer cytoskeletal pathology, Proc. Natl. Acad. Sci. U.S.A. 83 (1986) 4913–4917.

[6] C.M. Wischik, M. Novak, P.C. Edwards, A. Klug, W. Tichelaar, R.A. Crowther, Structural characterization of the core of the paired helical filament of Alzheimer disease, Proc. Natl. Acad. Sci. U.S.A. 85 (1988) 4884–4888.

[7] H. Wille, G. Drewes, J. Biernat, E.M. Mandelkow, E. Mandelkow, Alzheimer-like paired helical filaments and antiparallel dimers formed from microtubule-associated protein Tau in vitro, J. Cell Biol. 118 (1992) 573–584.

[8] O. Schweers, E.M. Mandelkow, J. Biernat, E. Mandelkow, Oxidation of cysteine-322 in the repeat domain of microtubule-associated protein tau controls the in vitro assembly of paired helical filaments, Proc. Natl. Acad. Sci. U.S.A. 92 (1995) 8463–8467.

[9] M. Goedert, R. Jakes, M.G. Spillantini, M. Hasegawa, M.J. Smith, R.A. Crowther, Assembly of microtubule-associated protein Tau into Alzheimer-like filaments induced by sulphated glycosaminoglycans, Nature 383 (1996) 550–553.

[10] K. Bhattacharya, K.B. Rank, D.B. Evans, S.K. Sharma, Role of cysteine-291 and cysteine-322 in the polymerization of human Tau into Alzheimer-like filaments, Biochem. Biophys. Res. Commun. 285 (2001) 20–26.

[11] E. Akoury, M. Pickhardt, M. Gajda, J. Biernat, E. Mandelkow, M. Zweckstetter, Mechanistic basis of phenothiazine-driven inhibition of Tau aggregation, Angew. Chem. Int. Ed Engl. 52 (2013) 3511–3515.

[12] B. Trinczek, J. Biernat, K. Baumann, E.M. Mandelkow, E. Mandelkow, Domains of Tau protein, differential phosphorylation, and dynamic instability of microtubules, Mol. Biol. Cell. 6 (1995) 1887–1902.

[13] A. Schneider, J. Biernat, M. von Bergen, E. Mandelkow, E.M. Mandelkow, Phosphorylation that detaches Tau protein from microtubules (Ser262, Ser214) also protects it against aggregation into Alzheimer paired helical filaments, Biochemistry (Mosc.) 38 (1999) 3549–3558.

[14] E. Chang, S. Kim, K.N. Schafer, J. Kuret, Pseudophosphorylation of Tau protein directly modulates its aggregation kinetics, Biochim. Biophys. Acta. 2011 (1814) 388–395.

[15] A. Abraha, N. Ghoshal, T.C. Gamblin, V. Cryns, R.W. Berry, J. Kuret, et al., C-terminal inhibition of Tau assembly in vitro and in Alzheimer's disease, J. Cell Sci. 113 (Pt 21) (2000) 3737–3745.

[16] T.C. Gamblin, R.W. Berry, L.I. Binder, Tau polymerization: role of the amino terminus, Biochemistry (Mosc.) 42 (2003) 2252–2257.

[17] C. Fauquant, V. Redeker, I. Landrieu, J.-M. Wieruszeski, D. Verdegem, O. Laprévote, et al., Systematic identification of tubulin-interacting fragments of the microtubule-associated protein Tau leads to a highly efficient promoter of microtubule assembly, J. Biol. Chem. 286 (2011) 33358–33368.

[18] J. Chen, Y. Kanai, N.J. Cowan, N. Hirokawa, Projection domains of MAP2 and Tau determine spacings between microtubules in dendrites and axons, Nature 360 (1992) 674–677.

[19] V. Daebel, S. Chinnathambi, J. Biernat, M. Schwalbe, B. Habenstein, A. Loquet, et al., β-Sheet core of Tau paired helical filaments revealed by solid-state NMR, J. Am. Chem. Soc. 134 (2012) 13982–13989.

[20] M. von Bergen, P. Friedhoff, J. Biernat, J. Heberle, E.M. Mandelkow, E. Mandelkow, Assembly of Tau protein into Alzheimer paired helical filaments depends on a local sequence motif ((306)VQIVYK(311)) forming beta structure, Proc. Natl. Acad. Sci. U.S.A. 97 (2000) 5129–5134.

[21] M. von Bergen, S. Barghorn, L. Li, A. Marx, J. Biernat, E.M. Mandelkow, et al., Mutations of Tau protein in frontotemporal dementia promote aggregation of paired helical filaments by enhancing local beta-structure, J. Biol. Chem. 276 (2001) 48165–48174.

[22] L. Amniai, G. Lippens, I. Landrieu, Characterization of the AT180 epitope of phosphorylated Tau protein by a combined nuclear magnetic resonance and fluorescence spectroscopy approach, Biochem. Biophys. Res. Commun. 412 (2011) 743–746.

[23] A. Sillen, A. Leroy, J.-M. Wieruszeski, A. Loyens, J.-C. Beauvillain, L. Buée, et al., Regions of tau implicated in the paired helical fragment core as defined by NMR, Chembiochem Eur. J. Chem. Biol. 6 (2005) 1849–1856.